

RSC Advances



This is an *Accepted Manuscript*, which has been through the Royal Society of Chemistry peer review process and has been accepted for publication.

Accepted Manuscripts are published online shortly after acceptance, before technical editing, formatting and proof reading. Using this free service, authors can make their results available to the community, in citable form, before we publish the edited article. This *Accepted Manuscript* will be replaced by the edited, formatted and paginated article as soon as this is available.

You can find more information about *Accepted Manuscripts* in the [Information for Authors](#).

Please note that technical editing may introduce minor changes to the text and/or graphics, which may alter content. The journal's standard [Terms & Conditions](#) and the [Ethical guidelines](#) still apply. In no event shall the Royal Society of Chemistry be held responsible for any errors or omissions in this *Accepted Manuscript* or any consequences arising from the use of any information it contains.

Band-gap tuning of graphene by Be doping and Be, B co-doping: A DFT study

Saif Ullah¹, Akhtar Hussain^{2,4*}, WaqarAdil Syed¹, Muhammad Adnan Saqlain³, Idrees Ahmad⁴, Ortwin Leenaerts⁵, and Altaf Karim⁶

¹Department of Physics, International Islamic University, Islamabad, Pakistan

²TPD, Pakistan Institute of Nuclear Science and Technology (PINSTECH), P. O. Nilore, Islamabad, Pakistan

³Department of Chemistry, Quaid-i-Azam University, Islamabad, Pakistan

⁴DNE, Pakistan Institute of Engineering and Applied Sciences, P. O. Nilore, Islamabad, Pakistan

⁵Department Fysica, Universiteit, Antwerpen, Groenenborgerlaan 171, B-2020 Antwerpen, Belgium

⁶COMSATS institute of information technology, Islamabad, Pakistan

Abstract

First-principles density functional theory (DFT) calculations were carried out to investigate the structural and electronic properties of beryllium (Be) doped and, Be and boron (B) co-doped graphene systems. We observed that not only the concentration of impurity atoms is important to tune the band-gap to some desired level, but also the specific substitution sites play a key role. In our system, which consists of 32 atoms, a maximum of 4 Be and, in the co-doped state, 2 Be and 3 B atom substitutions are investigated. Both dopants are electron deficient relative to C atoms and cause the Fermi level to shift downward (p-type doping). A maximum band gap of 1.44 eV can be achieved on incorporation of 4 Be atoms. The introduction of Be is more sensitive in terms of geometry and stability than B. However, in opening the energy gap, Be is more effective than B and N (nitrogen). Our results offer the possibility to modify the band gap of graphene sufficiently for utilization in diverse electronic device applications.

Key words: Graphene, band gap engineering, doping by Be and B, DFT, site dependent doping

*corresponding author's email: ahmohal@yahoo.com

1. Introduction

Graphene is a one-atom-thick sp^2 -hybridized monolayer of carbon atoms with a two-dimensional (2D) honeycomb lattice structure and forms the building block of all other graphitic materials, such as 0D fullerenes (Bucky ball), 1D nanotubes and 3D graphite [1-4]. In every graphene unit cell there are two non-equivalent carbon (C) atoms, which can be considered as two interweaving triangular sublattices, as shown in Figure 1. Graphene is an interesting material for scientists and engineers because of its potential applications in semiconductor nanoelectronics by virtue of its remarkable physical, electrical, and optical properties [3, 5-7]. Graphene has tremendous charge carrier mobility of about 10^6 cm²/Vs, which is 2-3 times greater than conventional semiconductors [8].

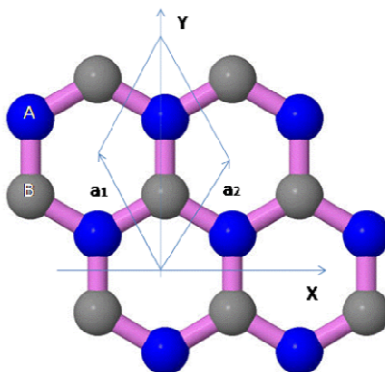


Figure 1: The unit cell of graphene consists of two non-equivalent sites (atoms) which are denoted by A and B where a_1 and a_2 denotes the primitive unit vectors.

Beside its exceptional properties, one serious issue in fabricating graphene-based transistors is its zero-gap character. For its use in semiconductor electronics, such as field-effect transistors (FETs), the opening of a band gap is very important for switching the devices off.

Consequently, the band-gap engineering [9] of graphene is an essential topic with regard to applications.

Fortunately, there are certain techniques by which the band structure of graphene can be engineered. An efficient technique to induce a band gap in graphene is to design superstructures of graphene-like nanoribbons [10, 11], quantum dots [12, 13], and nanomeshes [14]. All these superstructures lead to quantum confinement effects, which induce a band-gap. But the fabrication of these superstructures in a controllable way is still a major challenge. The fabrication of superstructures with homogeneous widths and well defined edges under 10 nm is very difficult to achieve with top-down approaches like lithography and etching. It is easier to achieve uniform structures through bottom-up approaches [15], but the extraction procedure of patterned nanoribbons is still an issue which need to be addressed. A simple process to induce a band-gap is to adsorb graphene on an epitaxial substrate such as SiC [16], Al₂O₃ [17], or BN [18]. However it is difficult to control the morphology and adsorption energies. One of the promising alternatives to open a band gap is the doping of graphene with suitable foreign atoms. Chemical and physical doping of graphene came into sight just after the isolation of graphene in 2004 [5] and is now turning into a sizzling area. Jing et al. [19] tested Graphene, inorganic graphene analogs (IGAs) and their composites for lithium ion batteries (LIB). An excellent review regarding to the doping of graphene and derived graphene nanoribbons, graphane, graphene oxide, fluorographene, graphyne, graphdiyne, and porous graphene has been presented in reference [20]. Graphene can be doped p-type (using Al, B, NO₂, H₂O, and F4-TCNQ as dopants) as well as n-type (using N, and alkali metals) [21-26]. These dopants significantly alter the electronic structure of graphene and induce a band-gap. Substitutional doping is usually achieved with boron (B) and nitrogen (N) atoms [27-33] because B and N are the closest neighbors to carbon (C).

It is desirable to dope graphene with light atoms like B, N, and oxygen (O) etc, to alter its electronic properties [23, 34, 35]. Another light atom is Be, which has 2 valence electrons and an electronic configuration $2s^2 2p^0$. Be is relatively lighter than B and obviously C atoms. At high melting temperatures of about 1500 K, Be atoms can be arranged to form an hexagonal close-packed (hcp) crystal structure. The synthesis of beryllium carbide (Be₂C), which is a hard material, can be achieved by heating Be and C at about 1173.15 K. Be can also be doped

in graphene by using chemical vapor deposition (CVD) techniques. Lee et al. investigated the adsorption of Be on fullerenes [36] and its capacity for hydrogen (H) storage has also been investigated with *ab-initio* calculations. These authors found that the aggregation of Be upon pure fullerene was energetically favored, causing the dissociation of H₂. DFT calculations were carried out by Ferro et al. [37] to investigate the absorption and diffusion of Be in graphite and the formation of Be₂C. The authors found that the high absorption of Be in graphite can lead to the creation of Be₂C. The structural and electronic properties of C_xBe_m clusters were examined by Patrick et al. [38] using first-principles. They argued that in bigger C_xBe_m structures, subclusters of Be atoms can be obtained.

In the current study, an attempt has been made to achieve band-gap engineering by substitutional doping with beryllium and Be along with B in graphene sheet by increasing the doping concentration slowly and systematically. The structural properties and electronic band structures of Be and Be/B codoped graphene are investigated using DFT calculations.

2. Details of Computation

First-principles calculations were performed with the Vienna *ab-initio* simulation package (VASP) based on density functional theory (DFT) [39]. The electron-ion interaction was described by the projected augmented wave (PAW) [40] method and the Perdew, Burke, and Ernzerhof (PBE) [41] version of the generalized gradient approximation (GGA) was adopted for the exchange and correlation parts of the electron-electron interactions. The plane-wave expansion of the wave functions was set to a kinetic energy cutoff of 450 eV. A slab model consisting of a 4 × 4 graphene supercell (32 atoms) was selected. Periodic boundary conditions are applied in all directions, so in order to avoid artificial interlayer interactions, the perpendicular distance between the layers was kept to 14 Å. Monkhorst-Pack grids are used to sample the Brillouin zone with 9 × 9 × 1 Γ -centered k mesh [42]. For the density of states (DOS) a denser k-point grid of 16 × 16 × 1 was used. Energy minimizations of the structures were performed until the total Hellmann-Feynman forces were smaller than 0.01 eV/Å. Cohesive energies were calculated using the following formula:

$$E_{coh} = \frac{E_{tot} - \sum n_x E_x}{N}$$

in which x stands for {C, Be, B}, E_x and n_x represent the atomic energy and the amount of atoms of type x , and N is the total number of atoms present in the system.

3. Results and Discussions

First, a geometry optimization was performed for the pristine graphene sheet, allowing all C atoms to relax. The lattice constant and C-C bond lengths of our optimized geometry were found to be 2.46 and 1.42 Å, respectively, as can be seen in Figure 2 (a). These parameters are in good accordance with experimental values [43]. The band structure of this optimized geometry was calculated and, as shown in Figure 2 (b), the conduction band minimum (CBM) and valence band maximum (VBM) are touching at the K point, forming the well-known Dirac cone. Our calculated band structure is in good agreement with previous studies in terms of gapless character and linear dispersion [3, 44].

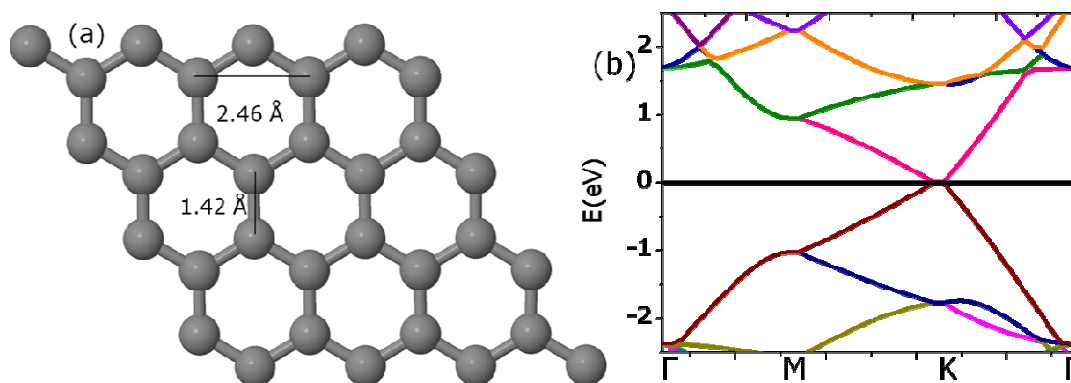


Figure 2: The optimized geometry of a 4×4 supercell of graphene is depicted in part (a). The calculated band structure of this geometry is shown in part (b). The Fermi level is put to zero.

The carbon atoms in graphene can be divided into two types according to the sublattice to which they belong, and are differentiated as A (blue) and B (red) sites as shown in Figure 3 (a). In addition to this division, we found that the obtained results also strongly depend on the specific configuration of atoms to be substituted by the dopants atoms. Therefore, we have chosen two configurations of C atoms to replace, namely rectangular (denoted as R1-R4 in Figure 3 (a)) and hexagonal (referred as H1-H4 in Figure 3 (b)). In rectangular configurations, which are located on A sublattice sites (hollow transparent spheres), the upper R2 and R4

sites in Figure 3 (a) are shifted by 2.46 Å (lattice constant) along the positive x-axis direction relative to the H2 and H4 positions of the hexagonal configuration (see Figure 3 (b)).

Our model of graphene retains a 2D character during geometry optimization process unless the doping concentration is increased to 12.5 % (4 Be atoms) and co-doping of Be and B to 15.625%. A Bader charge analysis [45-47] has been conducted for all the systems and it can be observed that the C atoms, being more electronegative than Be and B atoms, receive all the valence electrons. The charge transferred from either Be and/or B is largely localized on the C atoms lying in close proximity of the impurity atom.

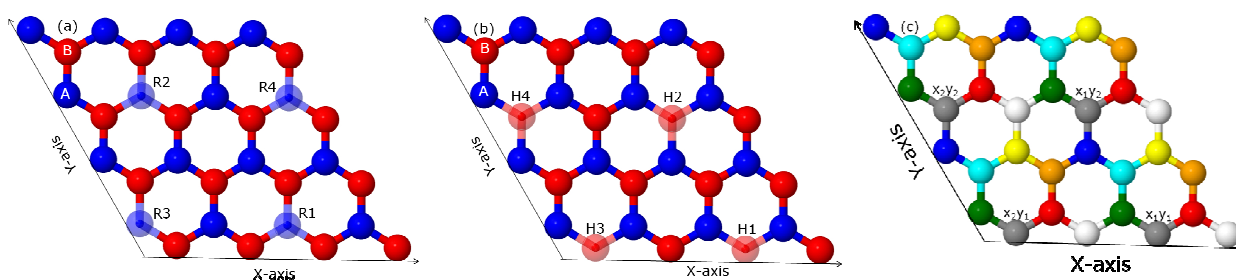


Figure 3: The rectangular doping of graphene is pictured in (a) (R1-R4 blue hollow spheres). The hexagonal doping configuration is given in part (b) indicated by red hollow spheres. The high symmetry of the hexagonal doping is depicted in part (c).

3.1 Rectangular Doping Configuration

In our graphene model, 1 to 4 C atoms were replaced systematically by Be atoms according to the rectangular configuration. The results are discussed in the following:

3.1.1. Doping with single Be atom

First, the graphene sheet was doped with a single Be atom making the concentration of Be 3.125 % (1/32) in host graphene. We performed a geometry optimization for this system until it reached the required accuracy. The two-dimensional structure of the system was retained after the optimization procedure. When Be is substituted in a graphene sheet, it binds with three C atoms through sp^2 hybridization. Due to the larger covalent radius of Be (102 pm) compared to C (75 pm), a substantial change in the bond lengths occurs. The adjoining Be-C

bond lengths are increased to 1.56 Å (where C-C bond lengths are 1.42 Å in graphene). This extension in Be-C bond lengths results in a decrease of C-C bond lengths in the proximity of the Be dopant. The nearby C-C bonds are reduced to 1.38 Å as depicted in Figure 4 (a). A similar extension of 1.48 Å [48] and 1.49 Å [23] in B-C bond lengths was found in earlier DFT studies. The covalent radii of B (85 pm) is larger than C and smaller than Be. Therefore, one can expect the Be-C bond length to be larger.

The cohesive energy of the system has been calculated to be -8.86 eV/atom which is lower than the cohesive energy of pristine graphene (-9.21 eV/atom). This value is in close agreement to the value (-9.20 eV/atom) reported by Rani and Jindal [48].

The charge transfer between C and Be atoms was calculated by means of Bader charge analyses [45-47]. Due to the higher electronegativity of C relative to Be, all the valence charge (2e) is transferred from Be to C atoms. A charge redistribution among the C atoms occurs with charges ranging from 3.758e to 4.515e. A higher value of charge is assigned to those C atoms which are located in the vicinity of the impurity atom. This is evident from the isosurface of the charge density distribution (see Figure 4 (b)). The white spots show charge depletion in that area. The reddish color between the C-C bonds is denser wherever charge accumulation occurs due to the charge gained (showing an increase in charge density), which is lost by impurity substitutions. However, in all the isosurface plots of doped graphene, this reddish intensity gets weaker when we move away from the impurity atoms. The charge accumulation on nearest neighboring C atoms bonded with Be can also clearly be seen in the form of white sparks in scanning tunneling microscopy (STM) images [49] (see Figure 4 (d)).

The total density of states (DOS) and the projected density of states (PDOS) calculations were performed in order to further investigate the role of dopant. The results are presented in Figure 4 e which indicate that the Be atom's $p_{x/y}$ orbitals (the three orbitals after sp_2 hybridization of the original p_x and p_y orbitals) strongly hybridize with the $p_{x/y}$ orbitals of carbon atoms. This strong overlapping between these p orbitals results in p - σ bonds formation near the Fermi level over an energy range from -0.5 eV to 0 eV. The p_z orbitals of carbon and beryllium overlap in conduction band resulting in π bond formation. The p_z orbitals of the C atoms are responsible for the DOS around the Dirac point, while the major portion of DOS at the Fermi level comes from all the $2p$ orbitals, but mainly from the $p_{x/y}$ orbitals close to the

dopant atom. Lastly, the DOS from C p_z orbitals contribute significantly over the wide energy range except at the energy gaps at Fermi level and around the Dirac point.

We also calculated the electronic band structure for this system. As Be atoms are electron deficient, a downward shift of the Fermi level of 0.81 eV below the Dirac point occurs. In other words, Be substitution leads to p-type doping. A similar shift of 0.70 eV due to B doping in graphene has already been reported in previous studies [21, 41]. Moreover, the additional symmetry of the two graphene sublattices breaks due to the introduction of Be impurity. The band structure of graphene is very sensitive to the sublattice symmetry and can be altered easily by changing this symmetry. This is well illustrated by an h-BN monolayer, which has different elements on its sublattices and, consequently, exhibits a large band gap [50]. In our case, a band gap of 0.46 eV is induced around Dirac point. Our results indicate that Be induced band-gaps are larger than those reported in previous investigations for single B and N atoms (see Table 1).

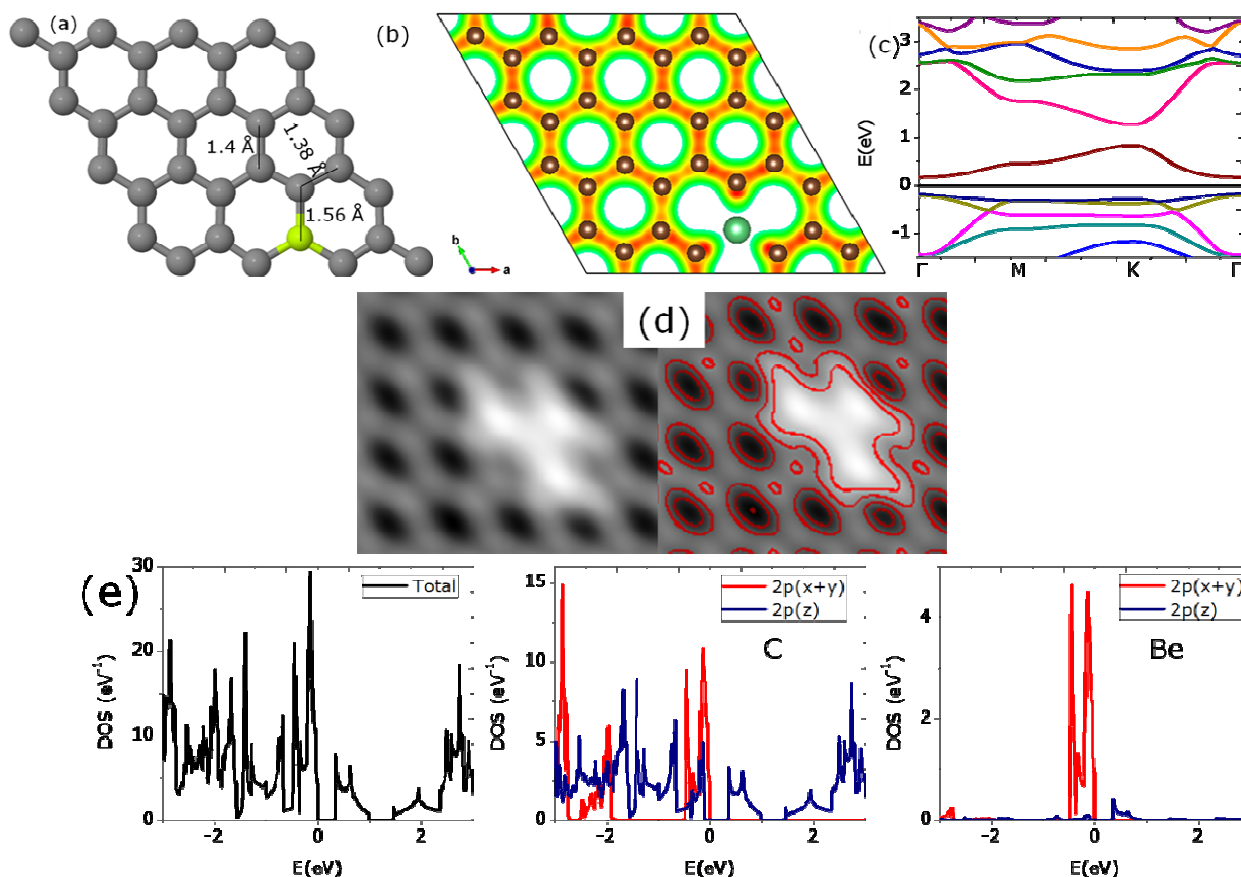


Figure 4: Optimized geometry of a graphene sheet doped with single Be atom and its iso-surface plot of charge density are given in part (a) and (b), respectively. The band structure diagram is depicted in (c). STM image [45] of the partial charge density is shown in part (e). Contour lines are drawn for clarity. The total and projected DOS are illustrated in part (e).

Table 1. A comparison of our results for Be with B and N doped graphene.

Reference	Dopants Type	Dopants Concentration (%)	Band-gap (eV)
Our work	Be	3.125	0.46
Ref.[23]	B	2	0.14
Ref.[23]	N	2	0.14
Ref.[48]	B	4	0.28
Ref.[48]	N	4	0.28

A minimal band gap of 0.4 eV is required for suitable on/off ratios for graphene-based transistors [51]. So the value of our calculated band gap meets this requirement. Furthermore, band gaps are generally underestimated by DFT [52, 53], so the actual value of the band gap is probably higher than our calculated value.

This remarkable result motivated us to carry out further calculations on graphene with an increasing concentration of dopants. Therefore, the graphene sheet is subsequently doped with 2, 3 and 4 Be-atoms, corresponding to dopant concentrations of 6.25, 9.75 and 12.5 %, respectively.

3.1.2 Doping with two Be atoms

In the following case two C atoms in graphene were replaced with Be atoms. After geometry optimization of the system, bond length increases among the various Be-C bonds were observed ranging from 1.55 to 1.57 Å, as shown in Figure 5 (a). As a result, the C-C bonds in the proximity of both the Be atoms were reduced in the range of 1.37 to 1.39 Å. The cohesive energy was found to be -8.49 eV/atom, which is smaller than for the case of a single Be atom.

The valence charge released by Be is gained by the neighboring C atoms as can be seen by the isosurface plot of the charge density (Figure 5 (b)). The charge redistribution on the C atoms ranges from 3.84 to 4.77e. The average charge gained per C atom was observed to be 0.133e. Band structure calculations reveal a band-gap opening of 0.58 eV (Figure 5 (c)). On increasing the Be concentration, the resulting increase in band gap is in agreement with previous studies for B and N doping [48].

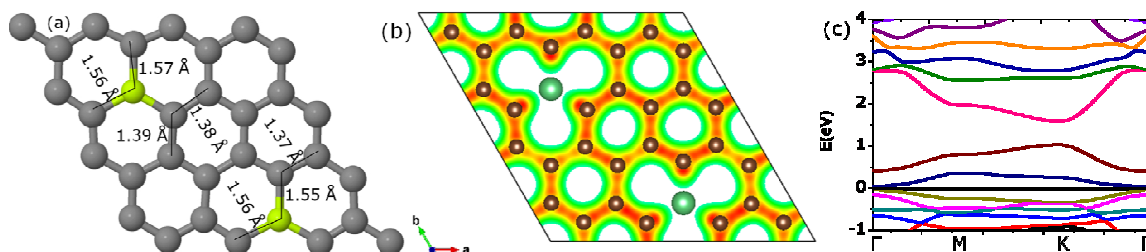


Figure 5: The parts (a), (b) and (c) show the optimized geometry, the resulting Iso-surface plot of the charge density and corresponding energy gap at Dirac point, respectively.

3.1.3 Doping with three Be atoms

The incorporation of three Be atoms leads to a concentration of 9.375 % of Be atoms in graphene. After geometry optimization, the neighboring Be-C bonds were stretched (ranging from 1.52 Å to 1.59 Å). Consequently, compression in next neighboring C-C bond lengths occurred. These C-C bond lengths reduced to a value as low as 1.36 Å in the locality of Be atoms. The cohesive energy was found to be -8.13 eV/atom, substantially lower than for pure graphene.

Charge rearrangement on C atoms ranges from 3.78e to 5.18e. A large part of the charge from the Be atoms was gained by the nearest C atoms as shown in the isosurface plot of the charge density in Figure 6 (b).

The electronic band structure is shown in Figure 6 (c). The calculated band gap was observed to be 0.69 eV. This gap is also higher than that reported in reference [48] for doping with 3 B and N atoms.

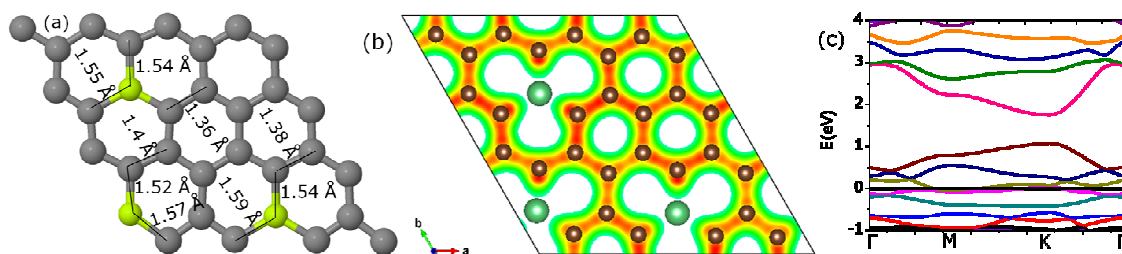


Figure 6: The optimized geometry of a graphene sheet doped with three Be atoms is depicted in part (a). Isosurface plot of the charge density is shown in part (b). The calculated band structure of this optimized geometry is given in part (c).

3.1.4 Doping with four Be atoms

The doping concentration was further increased to 12.5 % by replacing 4 C atoms by 4 Be atoms. The Be-C bonds in the neighborhood of Be atoms were either stretched to 1.56 or 1.52 Å. The corresponding compression in C-C bonds was observed to be as low as 1.36 Å. All bond variations resulting from the optimized geometry can be seen in Figure 7 (a). The calculated cohesive energy was significantly reduced to -7.75 eV/atom vs -9.21 eV/atom for pure graphene.

The charge relocation on the C atoms ranges from $3.91e$ to $4.69e$ and the average charge gained per C atom is $0.28 e$. The isosurface plot of the charge density, as shown in Figure 7 (b), shows that a major portion of the charge from the Be atoms is gained by neighboring C atoms. The band gap increases to 0.80 eV (see Figure 7 (c)) at the Dirac point.

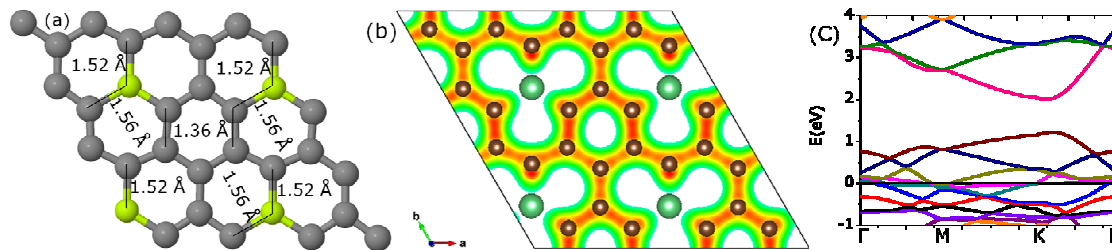


Figure 7: The optimized geometry of a graphene sheet doped with four Be atoms is depicted in part (a). Isosurface plot of the charge density is shown in part (b). The calculated band structure of the optimized geometry is given in part (c).

3.2 Hexagonal Doping Configuration

In addition to the impurity concentration, the actual configuration of the substituted C atoms is also an important factor that determines the value of the band gap. As detailed below, the band gap opening can be even higher for the same amount of Be impurities as above when different doping configurations are chosen.

3.2.1 Doping with two Be atoms

Two Be atoms were doped in the graphene sheet in such a way that both the atoms have same x-coordinate as shown in Figure 8 (a). We found that the neighboring Be-C bond lengths elongated up to 1.58 Å around the Be atoms after performing a geometry optimization. Consequently, shrinkage in the next-neighbor C-C bond lengths occurred upto 1.36 Å (Figure 8(a)). The calculated cohesive energy was found – 8.50 eV/atom for the present system. This value is very close to that calculated for 2 Be atoms (-8.49 eV/atom) in the rectangular case.

As in the previous calculations, a complete transfer of the valence charge occurs from both the Be atoms to graphene. Consequently, the range of charge redistribution on C atoms takes values between 3.75 and 4.80e which is wider than that of the rectangular case (3.84 to 4.77e). The charge relocation can be seen from the isosurface plot of the charge density which shows that C atoms in the proximity of Be atoms gain a large portion of the Be valence charge (Figure 8 (b)).

The calculated band gap is 0.6 eV, i.e. slightly larger than for the rectangular geometry (0.58 eV), with a slight shift away from the K and towards the M points of the Brillouin zone, as shown in Figure 8 (c).

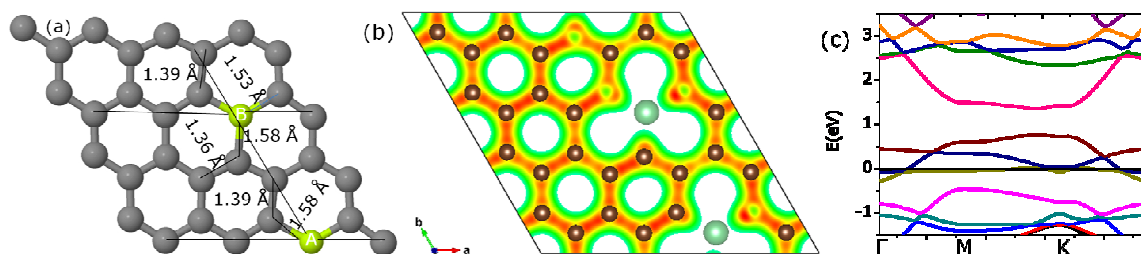


Figure 8: *The optimized geometry of a graphene sheet doped with two Be atoms (symmetrically) is depicted in part (a). Isosurface plot of the charge density is shown in part (b). The calculated band structure of this optimized geometry is presented in part (c).*

From these results, it appears that the geometry of the dopant sites is important (see Figure 3). Although the present structure has the same concentration of dopants, it is different from the system described in section 3.1.2, and consequently we observe differences in bond lengths, cohesive energy, and band gaps. The results show that in order to obtain a higher value of the band gap, the dopants should be incorporated in a trigonal way.

3.2.2 Doping with three Be atoms

Similar to that we did for the rectangular case, the replacement of Be atoms is now increased to 3. The neighboring Be-C bond lengths are elongated either to 1.54 or 1.6 Å after structural minimization. The expansion of the Be-C bonds is partly suppressed by the C-C bonds in close proximity to the Be atoms. These C-C bonds are contracted to 1.38 Å. The cohesive energy of the system was found to be -8.14 eV/atom which is similar to the value for rectangular case.

Charge readjustment on C atoms occurs in a range from 3.8e to 4.81e. The isosurface plot of the charge density shows that the excess charge transferred to graphene the sheet is gained by those C atoms which are bonded to Be atoms (see Figure 9 (b)).

The electronic band structure calculations reveal the opening of a band gap of 0.87 eV. The value of this calculated band gap is higher than the observed band gap of a graphene sheet doped with three Be atom in a rectangular way (0.69 eV). Thus a significant increase (0.18 eV) in band opening occurs just due to the symmetry of the Be dopants.

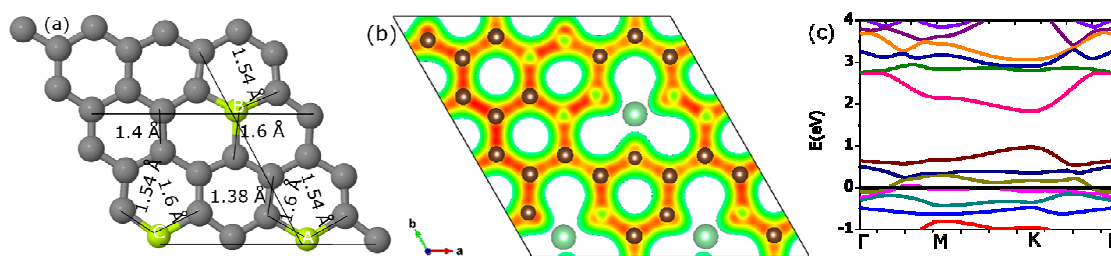


Figure 9: The optimized geometry of a graphene sheet doped with three (hexagonal) Be atoms is depicted in part (a). Isosurface plot of the charge density is shown in part (b). The calculated band structure of this optimized geometry is given in part (c).

3.2.3 Doping with four Be atoms

In order to find the maximum energy gap by incorporating the maximum tolerable impurity concentration, we replaced 4 C atoms with Be atoms in graphene as presented in Figure 10 (a). This configuration shows a perfect hexagonal symmetry as discussed in Figure 3 (b) and (c). The Be-C neighboring bond lengths around all the Be atoms are symmetrically elongated to 1.52 Å. At the same time, compression (1.37 Å) in the C-C bonds occurred. Cohesive energy of this system is -7.72 eV/atom, which is slightly lower than the rectangular doping of 4 Be atoms (-7.75 eV/atom)

As in the the previous cases, the whole valence charge transfers from Be to C (charge variation on C from 3.78e to 4.75e) according to a Bader analysis. The major portion of this charge is received by the neighboring C atoms of the Be as evidenced by the isosurface plot of the charge density in Figure 10 (b).

The electronic band structure shows a band gap opening of 1.44 eV. This value of the band gap is substantially larger (80 %) than the band-gap value of 0.80 eV which was obtained for the rectangular doping of the graphene sheet with four Be atoms. This is the highest value of the gap opening that we could obtain in our calculations. This corresponds to ideal hexagonal doping as the Be atoms actually form a 2×2 superlattice (see Figure 10 (a)). Furthermore, an important feature of such a high symmetric case is that the bond length extensions around the Be impurities and the accompanying compressions at all positions are all the same and induce a maximum effect to open up the band gap.

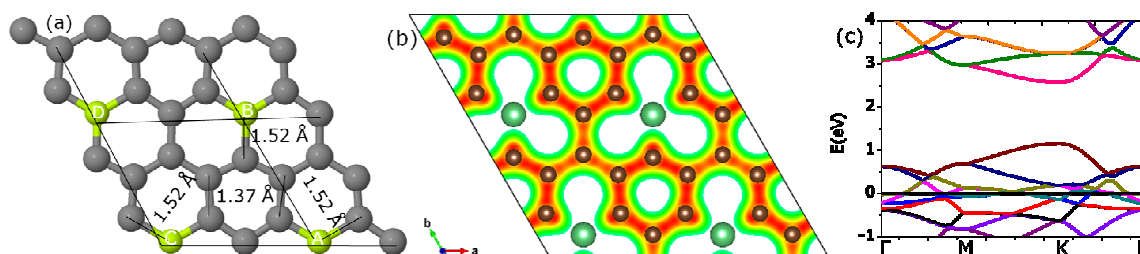


Figure 10: The optimized geometry of a graphene sheet doped with four Be atoms (symmetrically) is depicted in part (a). Isosurface plot of the charge density is shown in part (b). The calculated band structure of this optimized geometry is given in part (c).

From the above presented results it can be concluded that as the substitution of C atoms by Be atoms is increased from 1 to 4 in a rectangular way, the band gap increases linearly from 0.46 to 0.80 eV as depicted in the graph below (Figure 11). However, the band gap increases exponentially if the dopant substitutions are done in a hexagonal way. Although our computed values of the band gap for Be are substantially higher than the reported values for the same concentrations of B and N by Rani and Jindal [48], the trend of increasing band gap with increased doping concentration is similar. We tried to dope beyond this concentration, but the graphene structure could not be retained during the optimization procedure. Finally, we decided to use combinations of Be and B doping with varying concentration. The obtained results are discussed in the following subsection.

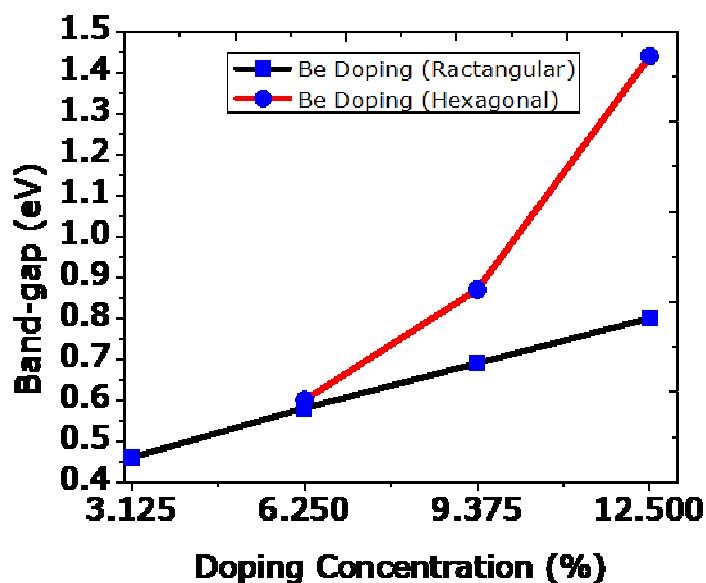


Figure 11: *The relation between Be doping concentrations and the corresponding calculated band gaps is plotted. The linear part of graph is for rectangular doping while the exponential part occurs as a result of C atom substitutions at hexagonal positions.*

3.3 Co-doping with Be and B

In this section, a combination of 1Be, 1B; 2Be, 2B and 2Be, 3 B (at various positions) atoms were substituted in the graphene as co-doping in graphene is reported in earlier studies [54, 55].

3.3.1 One Be, one B

Here two C atoms of graphene are replaced, one with a B atom and the other with a Be atom (corresponding to a dopant concentration of 6.25 %). The structural changes around the Be atom are observed to be the same as in case of single Be doping (section 3.1.1) as depicted in Figure 12 (a). The bond lengths changes are different around the B atom which is smaller compared to Be. The nearby B-C bonds are elongated to 1.48 Å, which is in a good agreement to earlier DFT studies [23, 48]. The next neighboring C-C bonds were reduced to either 1.41 or 1.4 Å. The B-C bonds are smaller than the Be-C bonds and larger than C-C bonds because the covalent radius of B (85 pm) is smaller than that of Be (102 pm) and larger than that of C (75 pm).

The cohesive energy of the system is -8.72 eV/atom. This model has a higher cohesive energy than that of a graphene sheet doped with two Be atoms (section 3.1.2, and 3.2.1) and lower than a graphene sheet doped with a single Be atom (section 3.1.1). This shows that B atoms have better chemistry with C atoms than Be.

Because of their respective electronegativity, the valence charge, from both Be (2e) and B (3e) is transferred to the carbon atoms, and is largely concentrated on those C atoms which are closest to the impurity atoms. However, the charge redistribution range (3.72e to 5.11e) has become wider compared to simple Be replacement. The C atoms in the vicinity of B gain a larger amount of charge compared to the C atoms bonded with Be because B loses 3e. This can be seen from the isosurface plot of the charge density as depicted in Figure 12 (b).

As a matter of fact, Be and B are both electron deficient and the Fermi level undergoes a downward shift of 1.13 eV below the Dirac point. This shift is higher than that computed for only Be doping (0.81 eV). As doping with Be and B in a graphene sheet leads in both case to hole doping, the system shows p-type behavior. As discussed above [50], the band structure can be engineered by breaking the sublattice symmetry of graphene. These dopants lead to an imbalance between the two sublattices of graphene and break the symmetry, resulting in a band gap opening of 0.49 eV.

The results from DOS and PDOS calculations of this system are depicted in part d of the Figure 12. The DOS around the Dirac point comes again from the p_z orbital of the C atoms. Contrary to the previous case of single Be doping; where the DOS at Fermi level was only due to $p_{x/y}$ orbitals of C and Be; here the C p_z orbitals are also contributing towards DOS in addition to $p_{x/y}$ orbitals of C and Be atoms. The main contribution to the DOS around the Fermi level comes from the C atoms bonded with the Be and B atoms. The Be atom's $p_{x/y}$ orbitals strong hybridization with the $p_{x/y}$ orbitals of carbon atoms results in p- σ bonds formation near the Fermi level over an energy range from -0.5 eV to 0 eV (similar as in sec. 3.1.1). Similarly, π bond formation just below the Dirac point comes from some overlapping of the p_z orbitals of carbon and beryllium atoms. The B atom has very small contributions to the DOS around the Fermi level. Nevertheless, the B $2p_{x/y}$ orbitals have strong hybridization with C $2p_{x/y}$ orbitals in the energy range from -2.5 to -1.7 eV, where p- σ bonds formation occurs. A minor overlapping can also be seen at some points between p_z orbitals of C and B in the valance and the conduction band region (Figure 12(d)).

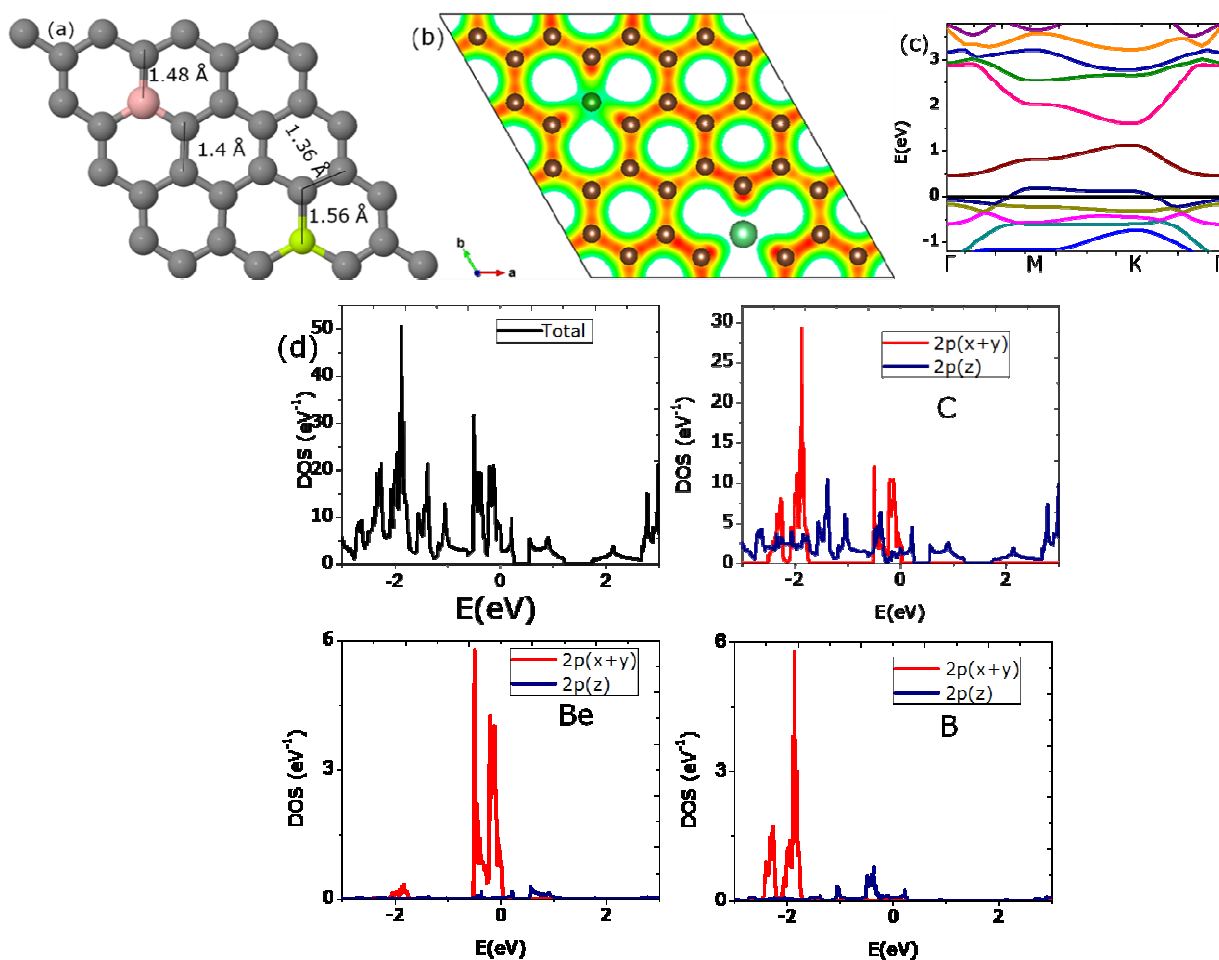


Figure 12: The optimized geometry of a graphene sheet co-doped with one Be and one B atom is shown in part (a). A charge density plot can be seen in part (b). The band structure of this optimized geometry is depicted in (c). Total as well as projected DOS are drawn in part (d).

3.3.2 Two Be, two B

Co-doping with two Be and two B atoms makes the total concentration of the impurities 12.5 % in the host graphene. The bonds around Be atoms are either enlarged to 1.57 or 1.52 Å after geometry optimization. The B-C bond lengths are found to be 1.44 Å, and 1.42 Å. The next neighboring C-C bonds in the vicinity of Be and B, on the other hand, are reduced to lower values (with a range from 1.37 to 1.39 Å). The changes in the bond length can be seen in Figure 13 (a). The system has a cohesive energy of -8.19 eV/atom, which is higher than the

cohesive energy of graphene doped with four Be atoms (-7.75 eV/atom). Thus C-B bonds are stronger relative to C-Be bonds.

The variation of the charge observed on the C atoms is in the range from $3.83e$ to $4.95e$. The average charge per C atom is increased to $0.36e$. Most of the charge which is transferred to graphene is acquired by those C atoms which are bonded with impurity atoms (Be, B). The neighboring C atoms of B attained greater amount of charge as compared to the C atoms bonded with Be atoms, as can be seen from the isosurface plot of the charge density (see Figure 13 (b)). The band structure calculations reveal a band-gap opening of 0.99 eV. The band structure diagram is depicted in Figure 13 (c). This value of the band gap is higher than in the case of doping with 4 Be atoms in a rectangular way and lower than in the hexagonal case.

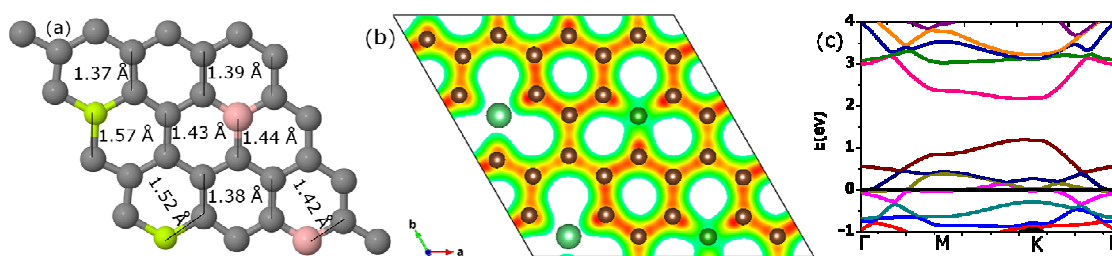


Figure 13: The optimized geometry of a graphene sheet co-doped with two Be atoms and two B atoms is depicted in part (a). Isosurface plot of the charge density is shown in part (b). The calculated band structure of this optimized geometry is given in part (c).

3.3.3.1 Two Be, three B (pattern I)

Co-doping with 2 Be and 3 B atoms makes the total concentration of the impurities 15.625 % in the host graphene. To incorporate the site effect, three mechanisms were investigated by varying the dopant position of one of the three B atoms. In pattern I, two Be atoms and two of the three B atoms are incorporated on the same sublattice while the third B atom is integrated on the other sublattice, as depicted in Figure 14 (a). The bonds in the proximity of the Be atoms are enlarged to either 1.52 or 1.57 Å after geometry optimization. Variations in the B-C neighboring bonds range from 1.41 to 1.5 Å (see Figure 14 (a)). The cohesive energy of this

model is -8.07 eV/atom, which is significantly higher than a graphene sheet doped with four Be atoms (-7.75 eV/atom). This shows that due to B insertion, the graphene structure is less destabilized than by Be substitution.

The charge redistribution on the C atoms is seen to range from $3.89e$ to $5.17e$. The isosurface plot of the charge density shows more local charge density near those C atoms which are bonded with B atoms as compared to those which are in the locality of Be atoms (see Figure 14 (b)). The average charge gain per C atom is $0.48e$. This is the highest value of charge gained per C atom.

A band-gap opening of 0.64 eV is observed. The value of this band gap is smaller than the band-gap value obtained for a graphene sheet co-doped with two Be atoms and two B atoms. This decrease is understandable because one of the B atoms was incorporated at a different sublattice compared to the other impurity atoms, which results in a smaller value of the band gap [48]. The band structure diagram is shown in Figure 14 (c).

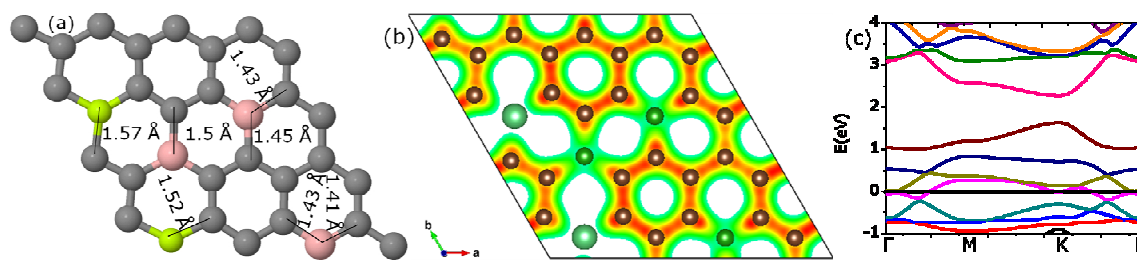


Figure 14: The optimized geometry of a graphene sheet co-doped with two Be atoms and three B atoms (pattern I) is depicted in part (a). Isosurface plot of the charge density is shown in part (b). The calculated band structure of this optimized geometry is given in part (c).

3.3.3.2 Two Be, three B (pattern II)

In the next part, the graphene sheet is doped with the same concentration of the same impurity atoms (as in upper case). However, the location of one B atom is changed such that the x-coordinates of all three B atom are the same. The relaxed Be-C neighboring bond lengths are stretched to values ranging from 1.51 to 1.57 Å as shown in Figure 15 (a). The B-C inter-

atomic bonds were found to be in the range of 1.44 to 1.46 Å. The cohesive energy of the system is -8.03 eV/atom a bit lower than the system discussed above.

The valence charge from the impurity atoms on the C atoms ranges from 3.87e to 5.95e. Two C atoms which are packed within B atoms have a larger value of accumulated charge (5.95e and 5.84e) as shown in the isosurface plot of the charge density (see Figure 15 (b)).

Band structure calculations show a band-gap opening of 0.96 eV. The value of the band gap is higher than the one observed for the above system because all the dopants are incorporated at same sublattice sites. The band structure diagram is depicted in Figure 15 (c).

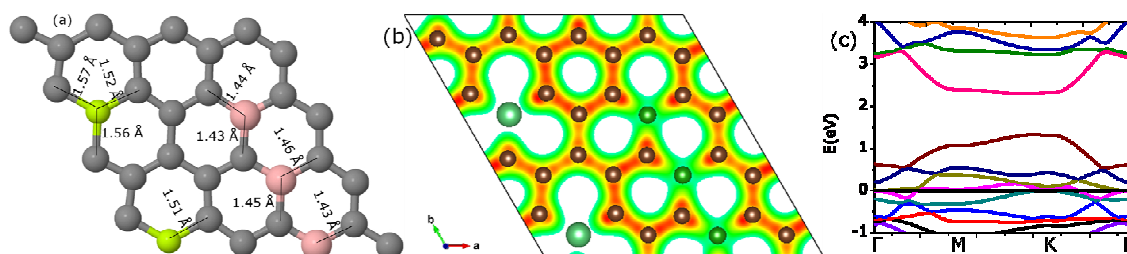


Figure 15: The optimized geometry of a graphene sheet co-doped with two Be atoms and three B atoms (pattern II) is depicted in part (a). Isosurface plot of the charge density is shown in part (b). The calculated band structure of this optimized geometry is given in part (c).

3.3.3.2 Two Be, three B (pattern III)

In this new configuration the position of one B atom is changed relative to the previous configuration, as shown in Figure 16 (a). This makes all impurity atoms reside on the same sublattice sites. The stretching of the Be-C bonds in the neighborhood of the Be atoms are in the range of 1.52 to 1.57 Å and the B-C bonds are lengthened up to 1.53 Å. The cohesive energy of the system is -8.06 eV/atom, similar to the above reported patterns I and II.

In this case we found a maximum charge of 7.09e on the C atom that is sandwiched between Be and B. This huge charge accumulation can also be nicely observed around the C atoms (the reddish line) near the lower Be atom in Figure 16 (b). Similarly, some C atoms retain a minimum charge of 2.63e. Thus the charge redistribution range is much wider relative to

previous cases. This fact is also reflected by the isosurface charge density plot in Figure 16 (b).

The value of the band gap is observed to be 1.12 eV as depicted in Figure 16 (c); the 2nd highest value we observed in this study. We can conclude that the present pattern with an impurity concentration of 15.625 % yields the maximum band gap value accompanied with maximum distortion in the geometric structure and charge relocation.

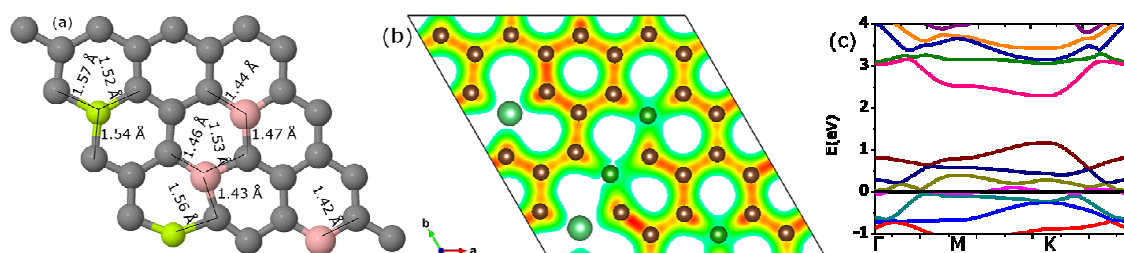


Figure 16: The optimized geometry of a graphene sheet co-doped with two Be atoms along with three B atoms (pattern III) is depicted in part (a). Isosurface plot of the charge density is shown in part (b). The calculated band structure of this optimized geometry is given in part (c).

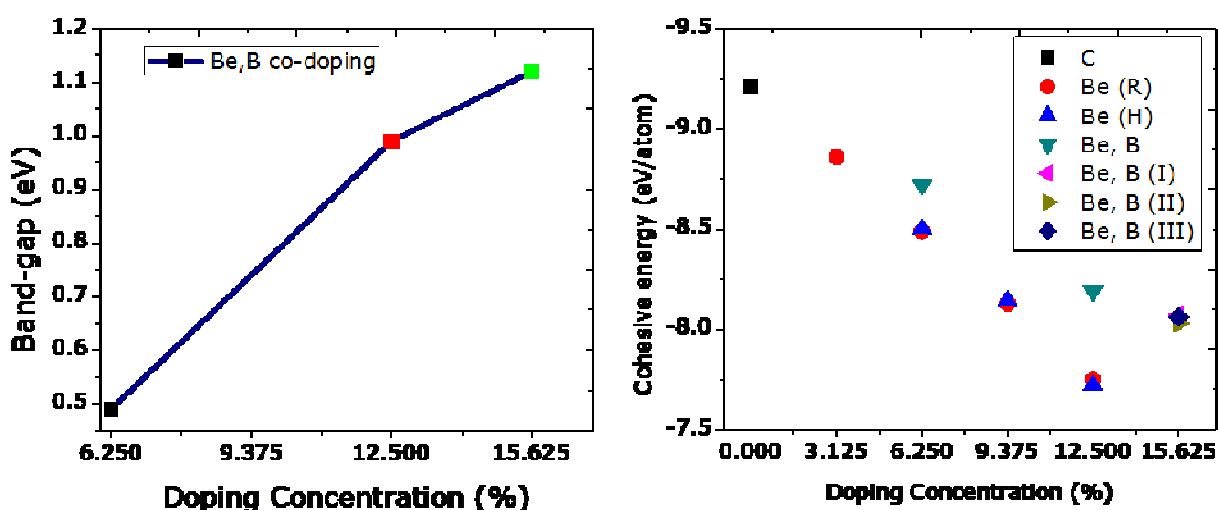


Figure 17: The relation between the band gap and co-doped concentration of Be and B (left panel). Only the pattern with the highest value of the band gap is shown here. In the right panel, the variation in cohesive energy with change in doping concentration and position is

depicted. The lowest cohesive energy corresponds to 4 Be atoms doping hexagonally against the highest value of (1.44 eV) energy gap.

All our results are summarized in Table 2. By increasing the impurity concentration, the value of the band gap increases but at the same time the value of the cohesive energy decreases, indicating a decrease in the stability of the structure as compared to a pristine graphene sheet. Graphene sheets co-doped with Be and B have higher cohesive energies as compared to that of Be doping only. This is because the covalent radius of B is closer that of C. Therefore, the bonds distort little as compared to Be, as illustrated by the variations of the bond lengths.

Table 2: Summary of the results obtained for Be, and, Be/B co-doping in graphene.

Dopants types	Concentration (%)	Pattern	Cohesive energy (eV/atom)	Band-gap (eV)
1 Be	3.125	Rectangular	- 8.86	0.46
2 Be	6.25	Rectangular	- 8.49	0.58
3 Be	9.375	Rectangular	- 8.13	0.69
4 Be	12.5	Rectangular	- 7.75	0.80
2 Be	6.25	Hexagonal	- 8.50	0.60
3 Be	9.375	Hexagonal	- 8.14	0.87
4 Be	12.5	Hexagonal	- 7.72	1.44
1 Be, 1 B	6.25	Same sublattice sites	- 8.72	0.49
2 Be, 2 B	12.5	Same sublattice sites	- 8.19	0.99
2 Be, 3 B	15.625	Different sublattice sites (Pattern I)	- 8.07	0.64
2 Be, 3 B	15.625	Same sublattice sites (pattern II)	- 8.03	0.96
2 Be, 3 B	15.625	Same sublattice sites (pattern III)	- 8.06	1.12

The cohesive energy of pristine graphene was calculated to be – 9.21 eV/atom.

4 Conclusions

First-principles DFT calculations were performed to investigate the structural and electronic properties of graphene systems doped with Be and co-doped with Be and B. Graphene was doped with Be atoms at different sites with varying concentration ranging from 1-4 per 4x4 graphene supercell. Be doping can significantly modify the electronic and structural properties of graphene. Replacement of a single C atom with a Be atom induces a band-gap of 0.46 eV, which seems sufficient for its use in transistor applications because graphene based FETs required a minimum band-gap of 0.4 eV [51] for useful on/off ratios. The shift in Fermi level indicates p-type doping. We studied two configurational symmetries for the dopants, namely rectangular and hexagonal. By an increase in the impurity concentration, a linear rise in the band gap was observed for rectangular doping. However, an exponential rise (max. value 1.44 eV) was observed for hexagonal doping, proving the superiority of hexagonal doping over rectangular (replacement sites dependency). Co-doping with a second species, namely B, with Be was investigated too. The structure remains intact up to 5 impurity atoms (2 Be and 3 B) in contrast to doping with only Be atoms in which case only 4 atoms can be tolerated. The position of the B atoms was varied in the structure to check for site-dependent variations in the energy gap. A wide variation in the band-gap from 0.64 to 1.12 eV was observed which illustrates the significance of the doping sites. A lower value of the energy gap resulting from co-doping indicates that pure Be is more efficient in inducing band gaps. It was also found that because of their higher electronegativity, C atoms receive all the valence electrons of the Be and B atoms. These electrons mainly accumulate on the C atoms closest to the Be and B atoms. Finally, increasing the impurity concentration leads to a decrease in cohesive energy of the system, indicating weakening the bonds. Our results offer the opportunity to tailor the electronic band structure of graphene up to desired level and allow its use in wide spread applications of electronic devices.

Acknowledgments

We are thankful to Dr. Arshad Farhan, Dr. Shafqat Hussain Shah and Dr. Saqib Javed for their time to time valuable suggestions and discussions.

References

- [1] P. R. Wallace, *Phys. Rev.*, vol. 71, p. 622, 1947.
- [2] R. Saito, G. Dresselhaus, and M. S. Dresselhaus, *Physical Properties of Carbon nanotubes*. London, UK: Imperial College Press, 1998.
- [3] A. K. Geim and K. S. Novoselov, *Nat. Mater.*, vol. 6, p. 183, 2007.
- [4] A. H. C. Neto, F. Guinea, N. M. R. Peres, K. S. Novoselov, and A. K. Geim, *Rev. Mod. Phys.*, vol. 81, p. 109, 2009.
- [5] K. S. Novoselov, A. K. Geim, S. V. Morozov, D. Jiang, Y. Zhang, S. V. Dubonos, I. V. Grigorieva, and A. A. Firsov, *Science*, vol. 306, p. 666, 2004.
- [6] K. S. Novoselov, A. K. Geim, S. V. Morozov, D. Jiang, M. I. Katsnelson, I. V. Grigorieva, S. V. Dubonos, and A. A. Firsov, *Nature*, vol. 438, p. 438, 2005.
- [7] A. K. Geim, *Science*, vol. 324, p. 1530, 2009.
- [8] E. V. Castro, H. Ochoa, M. I. Katsnelson, R. V. Gorbachev, D. C. Elias, K. S. Novoselov, A. K. Geim, and F. Guinea, *Phys. Rev. Lett.*, vol. 105, p. 266601, 2010.
- [9] K. S. Novoselov, *Nat. Mater.*, vol. 6, p. 720, 2007.
- [10] M. Y. Han, B. Ozyilmaz, Y. Zhang, and P. Kim, *Phys. Rev. Lett.*, vol. 98, p. 206805, 2007.
- [11] X. Li, X. Wang, L. zhang, S. Lee, and H. Dai, *Science*, vol. 319, p. 1229, 2008.
- [12] L. A. Ponomarenko, F. Schedin, M. I. Katsnelson, R. Yang, E. W. Hill, K. S. Novoselov, and A. K. Geim, *Science*, vol. 320, p. 356, 2008.
- [13] B. Trauzettel, D. V. Bulaev, D. Loss, and G. Burkard, *Nat. Phys.*, vol. 3, p. 192, 2007.
- [14] J. Bai, X. Zhong, S. Jiang, Y. Huang, and X. Duan, *Nat. Nanotechnol.*, vol. 5, p. 190, 2010.
- [15] J. Cai, P. Ruffieux, R. Jaafar, M. Bieri, T. Braun, S. Blankenburg, M. Muoth, A. Seitsonen, M. Saleh, X. Feng, K. Mullen, and R. Fasel, *Nature*, vol. 466, p. 470, 2010.
- [16] S. Y. Zhou, G.-H. Gweon, A. V. Fedorov, P. N. First, W. A. d. Heer, D.-H. Lee, F. Guinea, A. H. C. Neto, and A. Lanzara, *Nat. Mater.*, vol. 6, p. 770, 2007.
- [17] B. Huang, Q. Xu, and S. Wei, *Phys. Rev. B: Condens. Matter*, vol. 84, p. 155406, 2011.
- [18] G. Giovannetti, P. A. khomyakov, G. Brocks, P. J. Kelly, and J. v. d. Brink, *Phys. Rev. B: Condens. Matter*, vol. 76, p. 073103, 2007.
- [19] Y. Jing, Z. Zhou, C. R. Cabrera, and Z. Chen, *J. Mater. Chem. A*, vol. 2, p. 12104, 2014.
- [20] Q. Tang, Z. Zhou, and Z. Chen, *Nanoscale*, vol. 5, p. 4541, 2013.
- [21] P. A. Denis, *Chem. Phys. Lett.*, vol. 492, p. 251, 2010.
- [22] A. Lherbier, X. Blasé, Y.-M. Niquet, F. Triozon, and S. Roche, *Phys. Rev. Lett.*, vol. 101, p. 036808, 2008.
- [23] M. Wu, C. Cao, and J. Z. Jiang, *Nanotechnology*, vol. 21, p. 505202, 2010.
- [24] E. H. Hwang, S. Adam, and S. D. Sarma, *Phys. Rev. B*, vol. 76, p. 195421, 2007.
- [25] O. Leenaerts, B. Partoens, and F. M. Peeters, *Phys. Rev. B*, vol. 77, p. 125416, 2008.
- [26] H. Pinto, R. Jones, J. P. Goss, and P. R. Briddon, *J. Phys.:Condens. Matter*, vol. 21, p. 402001, 2009.
- [27] L. S. Panchakarla, K. S. Subrahmanyam, S. K. Saha, A. Govindaraj, H. R. Krishnamurthy, U. V. Waghmare, and C. N. R. Rao, *Adv. Mater.*, vol. 21, p. 4726, 2009.
- [28] D. Wei, Y. Liu, Y. Wang, H. Zhang, L. Huang, and G. Yu, *Nano Lett.*, vol. 9, p. 1752, 2009.
- [29] Y. Fan, M. Zhao, Z. Wang, X. Zhang, and H. Zhang, *Appl. Phys. Lett.*, vol. 98, p. 083103, 2011.
- [30] X. Fan, Z. Shen, A. Q. Liu, and J.-L. Kuo, *Nanoscale*, vol. 4, p. 2157, 2012.

- [31] A. K. Manna and S. K. Pati, *J. Phys. Chem. C*, vol. 115, p. 10842, 2011.
- [32] D. H. Wu, Y. F. Li, and Z. Zhou, *Theor Chem Acc*, vol. 130, p. 209, 2011.
- [33] Y. Li, Z. Zhou, P. Shen, and Z. Chen, *ACS Nano*, vol. 3, p. 1952, 2009.
- [34] F. Cervantes-Sodi, G. Csanyi, S. Piscanec, and A. C. Ferrari, *Phys. Rev. B*, vol. 77, p. 165427, 2008.
- [35] B. Biel, F. Triozon, X. Blase, and S. Roche, *Nano Lett.*, vol. 9, p. 2725, 2009.
- [36] H. Lee, B. Huang, W. Duan, and J. Ihm, *J. appl. Phys.*, vol. 107, p. 084304, 2010.
- [37] Y. Ferro, A. Allouche, and C. Linsmeier, *J. appl. Phys.*, vol. 113, p. 213514, 2013.
- [38] A. Patrick, P. Williams, and E. Blaisten-Barojas, *J. Mol. Struct.: Theochem*, vol. 824, p. 39, 2007.
- [39] G. kresse and J. Hafner, *Phys. Rev. B*, vol. 49, p. 14251, 1994.
- [40] P. E. Blochl, *Phys. Rev. B*, vol. 50, 1994.
- [41] J. P. Perdew, K. Burke, and M. Ernzerhof, *Phys. Rev. Lett.*, vol. 77, p. 3865, 1996.
- [42] H. Monkhorst and J. Pack, *Phys. Rev. B: Solid state*, vol. 13, p. 5188, 1976.
- [43] D. R. Cooper, B. D'Anjou, N. Ghattamaneni, B. Harack, M. Hilke, A. Horth, N. Majlis, M. Massicotte, L. Vandsburger, E. Whiteway, and V. Yu. (2012, Experimental Review of Graphene. [Review Article]. 2012, 56.
- [44] S. M. Kozlov, F. Vines, and A. Gorling, *Adv. Mater*, vol. 23, p. 2638, 2011.
- [45] W. Tang, E. Sanville, and G. Henkelmen, *J. Phys.: Condens. Matter*, vol. 21, p. 084204, 2009.
- [46] E. Sanville, S. D. Kenny, R. Smith, and G. Henkelman, *J. Comput. Chem.*, vol. 28, p. 899, 2007.
- [47] G. Henkelman, A. Arnaldsson, and H. Jonsson, *Comput. Mater. Science*, vol. 36, p. 354, 2006.
- [48] P. Rani and V. K. Jindal, *RSC Adv.*, vol. 3, p. 802, 2013.
- [49] D. E. P. Vanpoucke and G. Brocks, *Phys. Rev. B*, vol. 77, p. 241308(R), 2008.
- [50] X. Blase, A. Rubio, S. G. Louie, and M. L. Cohen, *Phys. Rev. B*, vol. 51, p. 6868, 1995.
- [51] F. Schwierz, *Nat. Nanotechnol.*, vol. 5, p. 487, 2010.
- [52] C. S. Wang and W. E. Pickett, *Phys. Rev. Lett.*, vol. 51, p. 597, 1983.
- [53] M. K. Y. Chan and G. Ceder, *Phys. Rev. Lett.*, vol. 105, p. 196403, 2010.
- [54] P. A. Denis, C. P. Huelmo, and F. Iribarne, *Computational and Theoretical Chemistry*, vol. 1049, p. 13, 2014.
- [55] P. A. Denis and C. P. Huelmo, *Carbon*, vol. 87, p. 106, 2015.